



# An Innovative Superconducting Magnetic Trap for Probing $\beta$ -decay in Plasmas

Giorgio Sebastiano Mauro<sup>1\*</sup>, Luigi Celona<sup>1</sup>, Giuseppe Torrisci<sup>1</sup>, Angelo Pidotella<sup>1</sup>, Eugenia Naselli<sup>1</sup>, Filippo Russo<sup>1</sup>, Maria Mazzaglia<sup>1</sup>, Alessio Galatà<sup>2</sup>, Fabio Maimone<sup>3</sup>, Ralf Lang<sup>3</sup>, Klaus Tinscher<sup>3</sup>, Domenico Santonocito<sup>1</sup> and David Mascali<sup>1</sup>

<sup>1</sup>Istituto Nazionale di Fisica Nucleare—Laboratori Nazionali del Sud (INFN-LNS), Catania, Italy, <sup>2</sup>Istituto Nazionale di Fisica Nucleare—Laboratori Nazionali di Legnaro (INFN-LNL), Legnaro, Italy, <sup>3</sup>GSI Helmholtzzentrum für Schwerionenforschung GmbH, Darmstadt, Germany

## OPEN ACCESS

### Edited by:

Giuseppe Verde,  
Universities and Research, Italy

### Reviewed by:

Kurt Ernst Stiebing,  
Goethe University Frankfurt, Germany

Sandor Biri,  
Institute for Nuclear Research  
(ATOMKI), Hungary

### \*Correspondence:

Giorgio Sebastiano Mauro  
mauro@lns.infn.it

### Specialty section:

This article was submitted to  
Nuclear Physics,  
a section of the journal  
Frontiers in Physics

Received: 29 April 2022

Accepted: 13 June 2022

Published: 04 July 2022

### Citation:

Mauro GS, Celona L, Torrisci G, Pidotella A, Naselli E, Russo F, Mazzaglia M, Galatà A, Maimone F, Lang R, Tinscher K, Santonocito D and Mascali D (2022) An Innovative Superconducting Magnetic Trap for Probing  $\beta$ -decay in Plasmas. *Front. Phys.* 10:931953. doi: 10.3389/fphy.2022.931953

The main aim of Plasmas for Astrophysics Nuclear Decays Observation and Radiation for Archaeometry (PANDORA) project is to build a compact and flexible magnetic plasma trap where plasma reaches a density  $n_e \sim 10^{11} - 10^{13} \text{ cm}^{-3}$ , and a temperature, in units of  $kT$ ,  $kT_e \sim 0.1 - 30 \text{ keV}$  in order to measure, for the first time, nuclear  $\beta$ -decay rates in stellar-like conditions. One of the most important aspects of an ECR Ion Source (ECRIS) is its magnetic system. In this paper, the numerical design of the PANDORA magnetic system is presented and validated by using the commercial simulators OPERA and CST Studio Suite, showing an excellent agreement between each other in terms of axial and radial field profiles. In conjunction to the magnetic system design, the overall injection system, including the microwave lines for plasma heating and the isotopes injection schemes with a focus on the developments of the oven for solid elements, has been conceived and will be discussed.

**Keywords:** electron cyclotron resonance ion source, magnetic system, numerical simulations, wave-plasma coupling, isotopes injection systems

## 1 INTRODUCTION

In the last decades, much experimental and theoretical efforts have been dedicated to investigate various possible scenarios which can influence nuclear decays rates. It has been predicted that sizeable variations in the decay properties can be observed in highly ionized nuclides. This would have a strong impact in the stellar nucleosynthesis where a hot plasma is formed and atoms can be found in different ionization states. In particular,  $\beta$ -decay properties of radioactive nuclei can be strongly affected by the high-temperature plasma of stellar environment. Few experimental evidences showing variations in the  $\beta$  decay rates as a function of the atomic ionization state have been collected, up to now, using storage rings. However, the storage ring approach is based on the investigations of a single charge state at a time: while clearly showing the role played by the high ionization state of an atom in the  $\beta$ -decay process, is not able to reproduce stellar-like conditions where, due to the high temperature of the plasma, a Charge State Distribution (CSD) of the ions is established. A totally new and challenging approach, based on the study of decays rates in a plasma whose conditions can mimic the hot stellar environment, has been conceived in the PANDORA (Plasmas for Astrophysics Nuclear Decays Observation and Radiation for Archaeometry) project Mascali et al. [1]. The main idea is to build a compact and flexible magnetic plasma trap (where plasma reaches a density  $n_e \sim 10^{11} - 10^{13} \text{ cm}^{-3}$ , and a temperature

$kT_e \sim 0.1\text{--}30$  keV) and use it to measure, for the first time, nuclear  $\beta$ -decay rates in stellar-like conditions. The decay rates of the radioactive ions will be measured through the detection of the  $\gamma$ -rays emitted by the  $\beta$ -decaying daughter nuclei, as a function of the charge state distribution of the in-plasma ions by varying plasma conditions. This task will be accomplished by an array of several Hyper-Pure Germanium (HPGe) detectors placed around the trap, in specific positions where holes are made in the cryostat structure to directly look into the plasma through thin aluminium windows. This new approach is expected to have a major impact in the study of nuclear-astronomy processes and cosmology.

The magnetic field, necessary for plasma confinement, will be produced by employing a superconducting magnetic system (as typical for ECR ion sources), discussed in **Sections 2** and **3**, consisting of six hexapole coils (for radial confinement) nested inside three solenoid coils (for axial confinement), i. e. a SEXT-IN-SOL configuration. This magnetic system configuration is called *minimum-B* and allows the confinement of a plasma located around the plasma chamber axis ( $z$  axis in the following), providing magnetohydrodynamical (MHD) equilibrium and stability. In **Section 4** an overview of the microwave injection system that will be used in PANDORA will be given. The source will operate by employing three microwave injection lines: two 18 GHz lines with 2.4 kW maximum output power and one 21 GHz line with 1.5 kW maximum output power. This configuration will allow to exploit the advantages of different injection schemes, such as multiple frequency heating and two-close-frequency heating, in order to increase the production of higher charge states and overall plasma stability. Finally, **Section 5** will discuss about the techniques to inject isotopes inside the magnetic trap and will report a preliminary study of neutral vapour diffusion inside the PANDORA chamber. This is a critical point since PANDORA will employ radioactive isotopes, usually available in limited amount and very expensive, so the injection efficiency needs to be maximized.

## 2 ECR ION SOURCES MAGNETIC SYSTEM

It is known that, for ECRISs, high charge state ions are primarily produced by sequential impact ionization, which means that the ions must remain in the plasma long enough (up to hundreds of ms) to reach high charge states. Therefore, one of the main parameters determining the performance of an ECRIS is the product of the plasma density,  $n_e$ , and ion confinement time  $\tau_i$ , called quality factor  $Q = n_e \tau_i$ . In general, source development has followed the semi-empirical scaling laws first proposed by Geller [2], which state that the plasma density scales with the square of the frequency  $n_e \approx \omega_{RF}^2$ . As the frequency increases, the magnetic fields have to be scaled accordingly to fulfill the resonant heating condition for the plasma electrons Gammino and Ciavola [3]. As a consequence, the ion confinement time increases: in fact, it is proportional to the value of the so called mirror ratio, i. e. the ratio between the maximum and

the minimum magnetic field value for the considered magnetic system. Furthermore, the ion confinement time increases with plasma chamber length (mirror length) and radius, so these two values need to be increased if the objective is to obtain the highest possible charge states Leitner [4]. **Figure 1** shows a typical magnetic field pattern (in module) generated using a minimum-B magnetic configuration. Usually, the performances of a magnetic system in terms of plasma confining capability are expressed by five magnetic field values: the value corresponding to the ECR,  $B_{ECR}$ , that depends on the heating frequency  $f_{RF}$ ; the maxima values at the injection and extraction sides of the trap,  $B_{inj}$  and  $B_{ext}$  respectively, along the plasma chamber axis; the minimum,  $B_{min}$ , usually located at a central position along the plasma chamber axis; the maximum generated by the sextupole at the plasma chamber inner walls,  $B_{hex}$ . For a frequency of 28 GHz  $B_{ECR}$  is 1 T and its value at other frequencies can be easily calculated from the equation:

$$B_{ECR} [T] = \frac{f_{RF} [GHz]}{28 [GHz]} \times 1 [T] \quad (1)$$

Then, the established field ratios can be calculated as

$$B_{inj}/B_{ECR} = 4 \quad (2)$$

$$B_{rad}/B_{ECR} = 2 \quad (3)$$

$$B_{ext} \approx 0.9 - 1.2 \times B_{rad} \quad (4)$$

$$0.4 < B_{min}/B_{ECR} < 0.8 \quad (5)$$

Some considerations can be made about the magnetic field values Leitner [4]. The optimum charge state is proportional to the average magnetic field as  $q_{opt} \propto B^{3/2}$ , so it is of our interest to increase the average confining field. The highest value of the magnetic field will be in correspondence of the injection and/or extraction axial coils inner surface, so during the numerical design of the magnetic system one has to be careful at not exceeding the threshold field values relative to the magnet material. In superconducting traps, special attention must be paid to the minimum field,  $B_{min}$ , that should be tuneable within a wide range of values: it has been experimental observed that, in order to obtain the highest electron density and to reach the optimal charge state, one has to have  $0.65 < B_{min}/B_{ECR} < 0.75$  Benitez et al. [5]; Mazzaglia et al. [6]; Neben et al. [7]. If this ratio exceeds the upper value, sudden non linear effects arise, increasing the plasma x-ray emission and thus the heat load on the cryostat.

## 3 NUMERICAL DESIGN OF THE PANDORA MAGNETIC TRAP

The requirements and considerations discussed in **Section 2** together with the necessity to have enough space for non-invasive diagnostic tools and for the array of  $\gamma$ -ray detectors Naselli et al. [8], allowed us to fix the plasma chamber dimensions (internal radius  $R_{CH\_IN} = 140$  mm and axial length  $L = 700$  mm) and RF pumping frequencies ( $f_{RF1} =$

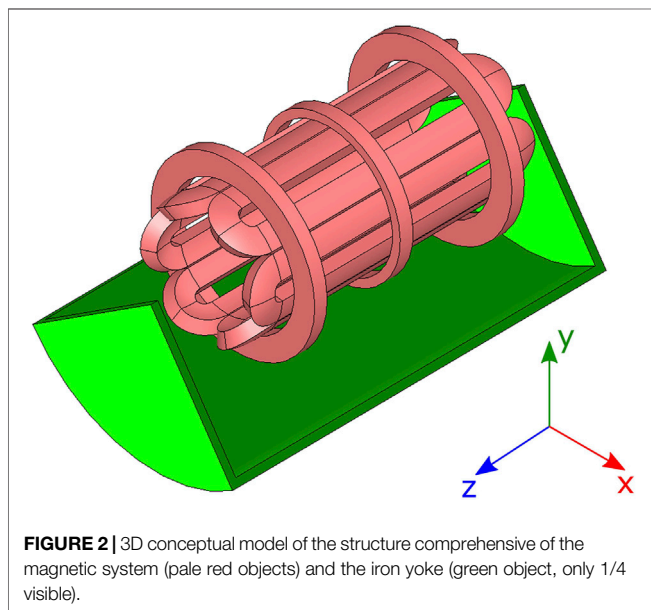
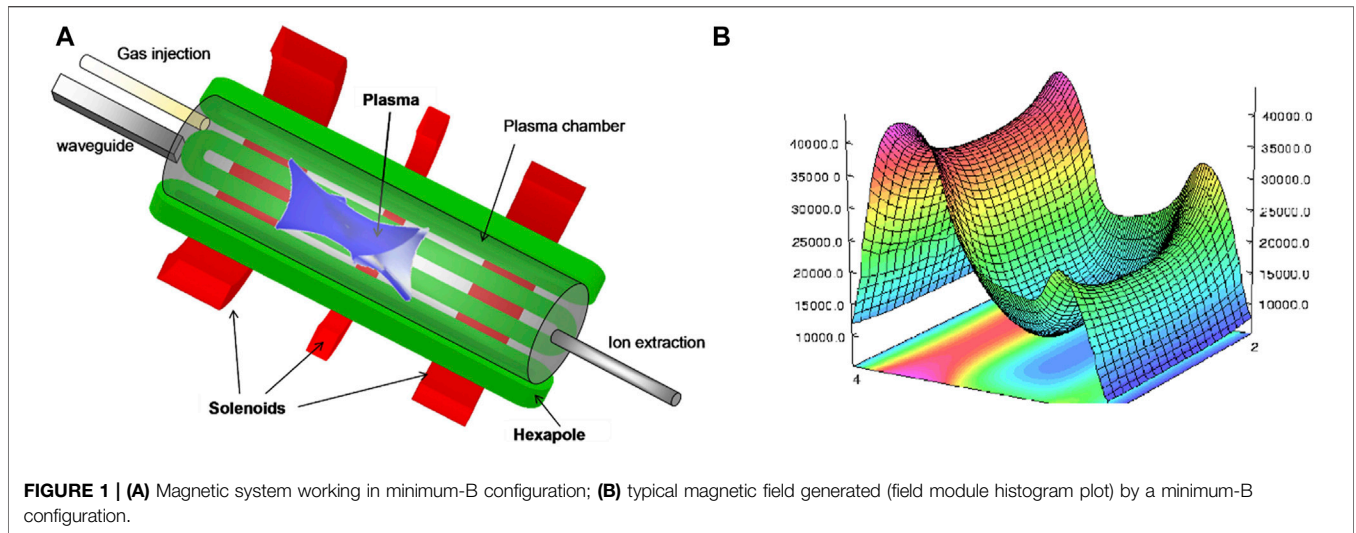


**TABLE 1 |** PANDORA magnetic field specifications and operative ranges.

Parameter	Value [T]
$B_{inj}$ max @ $z = 350$ [mm]	3
$B_{inj}$ operative range	1.7–3
$B_{ext}$ max @ $z = -350$ [mm]	3
$B_{ext}$ operative range	1.7–3
$B_{min}$ @ $z = 0$ [mm]	0.4
$B_{hex}$ @ $R_{CH\_IN}$	1.6

18 GHz,  $f_{RF2} = 21$  GHz). Taking into account these values, the PANDORA magnetic system field specifications have been obtained. The superconducting system, whose 3D conceptual model is shown in **Figure 2**, is composed by

three axial coils and six radial coils: the field values as well as the operative ranges are reported in **Table 1**. The structure has been simulated with the commercial softwares OPERA<sup>®</sup> and CST Studio Suite<sup>®</sup>. The simulated OPERA model and the employed coil dimensions are reported in **Figure 3** and **Table 2**. In the model, the material of the superconducting coils and of the sextupole is Niobium-Titanium alloy (NbTi). The simulated model takes also into account a 25 mm thick iron yoke (ARMCO<sup>®</sup> iron), distant 20 mm from the injection and extraction coils outer radius, employed to minimize the stray field that could otherwise interfere with the external detectors. The realized superconducting coils assembly will be encased inside a cryostat that will include a central warm bore for plasma chamber insertion.

The axial and radial magnetic field profiles are reported in **Figure 4** and **Figure 5**, scaled for the case  $f_{RF} = 18$  GHz.

Numerical simulations have also been performed to identify the positions of the magnetic branches that need to be avoided when placing the array of  $\gamma$ -ray detectors. In fact, in these positions a rather strong Bremsstrahlung radiation generated on the plasma chamber wall is present due to the intense flux of electrons escaping the magnetic trap, leading to a high background rate on the detectors and thus limiting their performances. The magnetic branches are clearly visible in **Figure 6**, which shows the  $|B|$  vector plots (normalized to the value of 2.7 T) in the  $xy$  plane at the axial positions  $z = -100, 0, 100$  mm.

By employing the magnetic field profile obtained in the simulations, the distribution of lost electrons on chamber walls due to the magnetic branches has been calculated through the use of a MATLAB particle mover code. **Figure 7** shows the obtained lost electrons mask on chamber walls. The numerical study matches the expected branches position given from CST and at the same time provides a lower boundary thickness of particle loss regions along the branches. These information are relevant for both designing the size of the bias-disk foreseen at the chamber

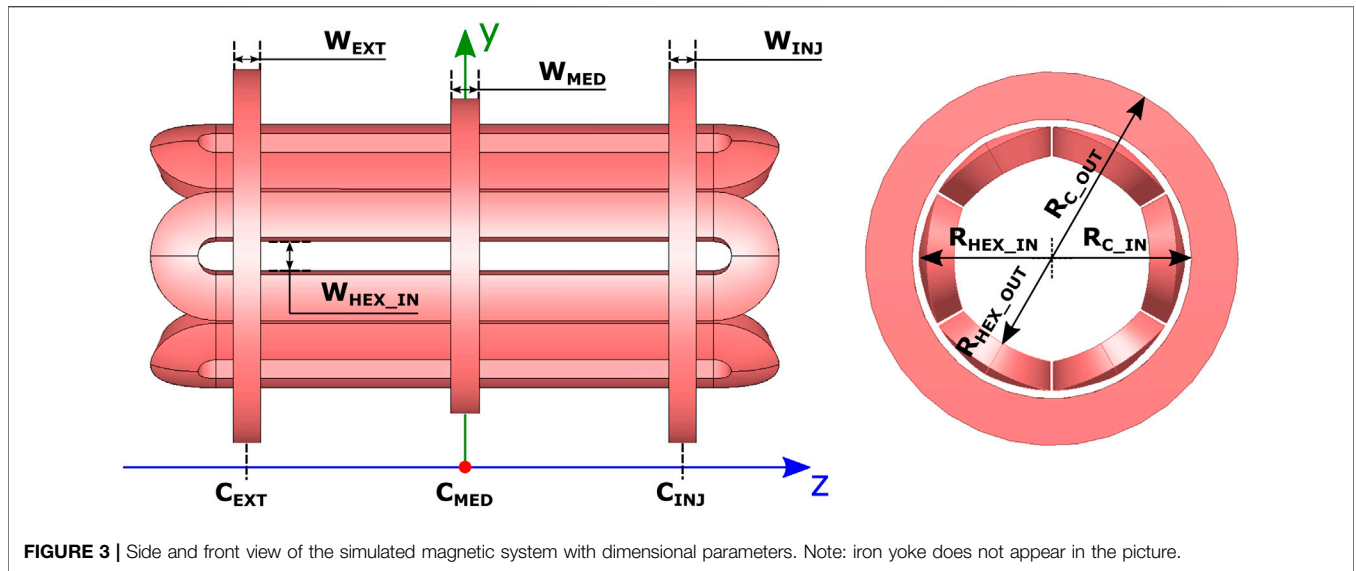


**FIGURE 3** | Side and front view of the simulated magnetic system with dimensional parameters. Note: iron yoke does not appear in the picture.

**TABLE 2** | Simulated geometrical dimensions of the coils composing the magnetic trap.

**Axial Coils**

Parameter	Description	Value [mm]
$R_{C\_IN}$	Coil inner radius (inj, med, ext)	225/225/225 [mm]
$R_{C\_OUT}$	Coil outer radius (inj, med, ext)	300/253/300 [mm]
$C_{INJ,MED,EXT}$	Coil center (inj, med, ext)	-350/0/350 [mm]
$W_{INJ,MED,EXT}$	Coil width (inj, med, ext)	44/46/44 [mm]

**Hexapole**

Parameter	Description	Value [mm]
$R_{HEX\_IN}$	Hexapole inner radius	165 [mm]
$R_{HEX\_OUT}$	Hexapole outer radius	212 [mm]
$W_{HEX\_IN}$	Hexapole coil inter-space width	78 [mm]

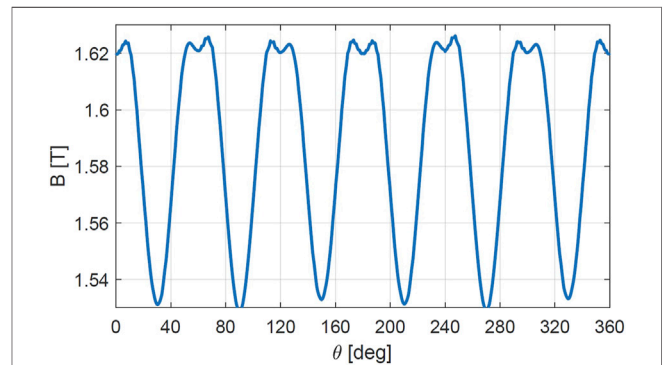


**FIGURE 5** | Magnetic field module,  $|B|$ , along a circumference of radius  $R_{CH\_IN} = 140$  mm (plasma chamber inner radius) and axial position  $z = 0$  mm.

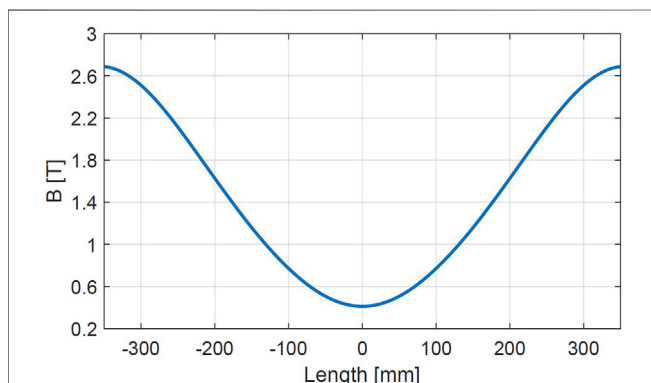


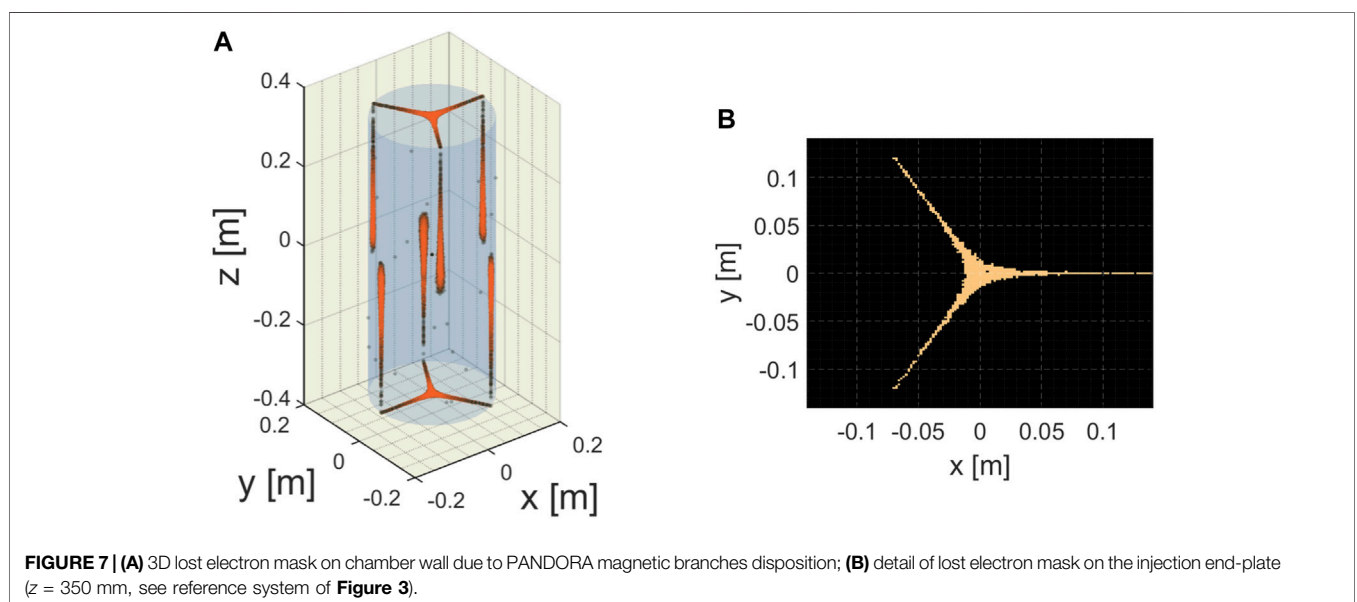
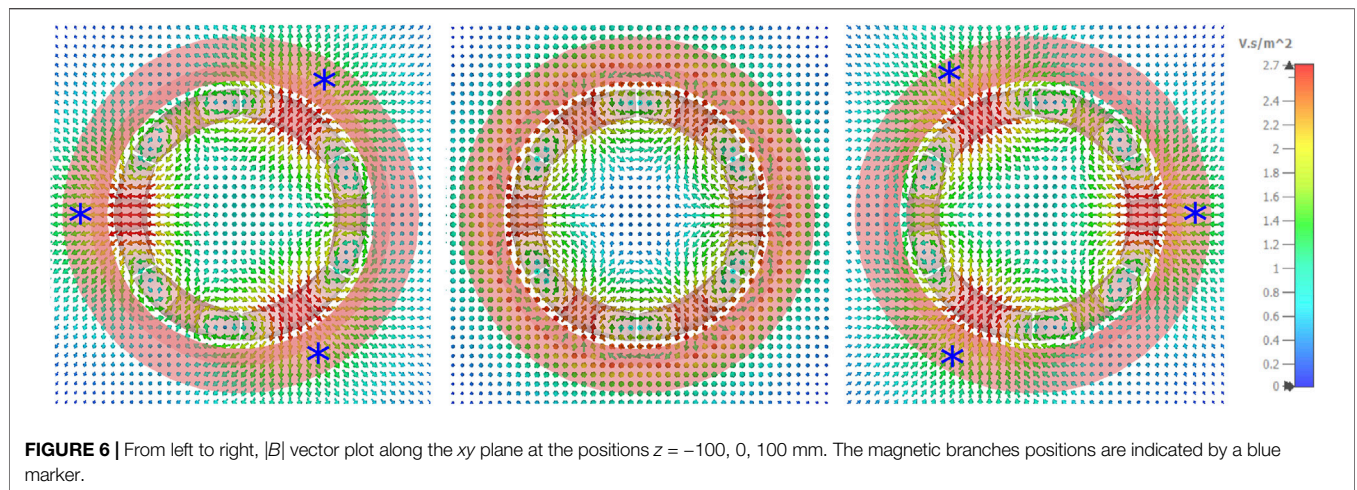
**FIGURE 4** | Magnetic field module,  $|B|$ , along plasma chamber z-axis for pumping frequency  $f_{RF} = 18$  GHz.

injection side, and to find the optimal position for plasma diagnostics, microwave injection waveguides along the

injection flange, as well as for the isotope injection systems (e. g., resistive oven), as will be discussed in the next sections.

### 4 THE MICROWAVE INJECTION SYSTEM

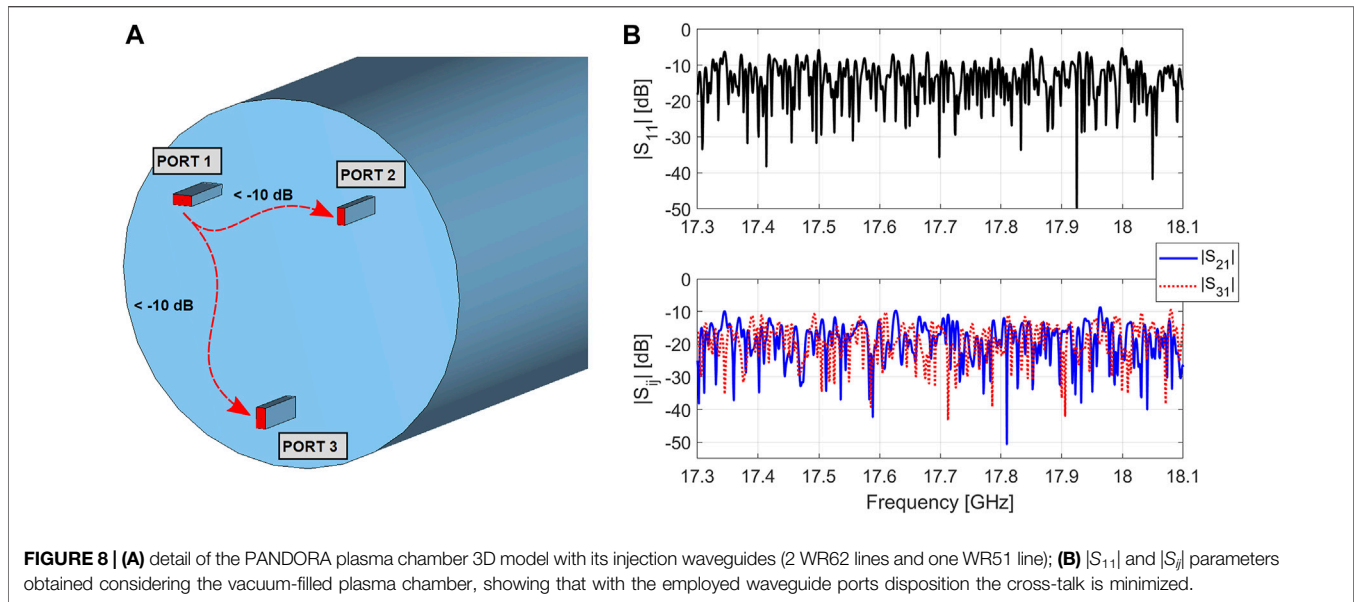
The source performances in terms of charge states and extracted currents has been explained by taking into account the different patterns of the electromagnetic field that are excited into the cavity, for a specific frequency (or set of frequencies) Mascali et al. [9]; Gammino et al. [10]. An improved coupling between microwaves and plasma is a key factor to design more powerful electron cyclotron resonance and microwave ion sources Hitz et al. [11]; Zhao et al. [12]; Xie et al. [13]; Guo et al. [14]; Mauro et al. [15]. As said, the electron density is proportional to the square of the microwave pumping frequency: the higher the frequency the higher the microwave power the source plasma can absorb before the onset of instabilities. However, taking



into account Geller scaling laws for the magnetic field, a limit arise in terms of magnetic system manufacturability. Multiple frequency heating improves plasma stability and source performance. Historically, this can be considered the first non-conventional method of plasma heating outside the scheme traced by the standard model. Since 1994, the so-called two-frequency heating (TFH) has been used Vondrasek [16] to improve the highly charged ions production by feeding the plasma with two (or more) electromagnetic waves at different frequencies instead of one. From the above considerations and also considering the non conventional PANDORA plasma chamber dimensions with respect to the state of the art ECRISs in the world Leitner [4], it has been decided that the RF injection system will be composed of three lines by employing:

- two Klystrons with 17.3–18.1 GHz operating bandwidth and 2.4 kW maximum output power;
- one Klystron with 21–22 GHz operating bandwidth and 1.5 kW maximum output power.

This configuration will allow to operate with different microwave injection schemes, and in particular: 1) single-frequency mode by employing only one amplifier; 2) two-frequency heating and two-close-frequency heating (TCFH) modes, also with the possibility to vary the power ratio between two microwave amplifiers; 3) three-frequency-heating mode by simultaneously employing the three amplifiers. A final consideration can be made about the selected total microwave power that could be delivered to the PANDORA plasma chamber. Its cooling is an engineering challenge: in all the high performance ECR ion sources operating today, the maximum



microwave power density (referred to plasma chamber volume) that can be coupled into the source is usually between 1.38 kW/L and 2.1 kW/L before a performance plateau is reached Lyneis et al. [17]. Considering a target power density of 1.38 kW/L and considering the PANDORA plasma chamber volume ( $\sim 40$  l), an impractical required total microwave power would result in order to obtain the maximum charge state intensity. This issue can be overcome if we consider 100% of power density coupled to the volume enclosed by the resonance surface (the plasma volume), equal to  $\sim 3$  l in the case of  $f_{RF} = 21$  GHz. In this case, a total required microwave power  $P_{coupled} \approx 4$  kW is obtained: this value is compliant with the planned total amount of power delivered by the three klystrons, which is close to 6 kW. Such a power allows to obtain the charge state intensities needed for the experimental program. The PANDORA waveguide injection system has been initially simulated in CST by considering a vacuum-filled cavity in order to choose the correct waveguide positions and reciprocal orientation angle, with the aim at minimizing the cross-talk between each other and to avoid the magnetic branches (i. e. where the plasma hits the chamber injection end-plate, see **Figure 7**). As an example, **Figure 8** shows the waveguides positioning scheme as well as the reflection ( $|S_{11}|$ ) and transmission ( $|S_{ij}|$ ) parameters when only port 1 (WR62 waveguide) is enabled. From the picture it can be seen that, with the proposed configuration, the waveguide ports cross-talk is minimized, that is  $|S_{ij}| < -10$  dB. By looking at the  $|S_{11}|$  it can also be noticed that a high number of well adapted modes is excited inside the empty cavity.

## 5 ISOTOPES INJECTION TECHNIQUES

Besides the challenges encountered in the design of the magnetic and microwaves injection systems, a special attention was dedicated to the identification of the techniques to inject the various elements of interest inside the magnetic trap. The experiments carried out within PANDORA will involve, in

fact, the use of radioactive isotopes, usually available in limited amount and very expensive: for this reason, it is mandatory to choose the most efficient injection technique, not only in terms of percentage of atoms effectively introduced inside the plasma, but also of ease and speed of preparation, in particular in the case of solid elements (radioactive elements could lead to a dose for the operator during their handling). The techniques will be employed within PANDORA derive directly from the experience made with ECRIS operation with solid elements: in this case, it is necessary to create first a neutral vapour, or an ejection of neutral particles towards the plasma. Neutral vapours of solid elements are usually obtained using small ovens installed just outside the plasma and heated by a DC/AC (resistive) or radiofrequency (RF) current Brown [18]. In general, resistive ovens can be used for elements whose vapor pressure reaches  $10^{-2}$  mbar at a temperature  $T \leq 2000$  °C. They consist in a crucible with a very thin filament wrapped on it: the crucible is filled with the compound to evaporate and is heated by letting the current flow through the filament. Such kind of ovens are usually very small and are mounted inside the ECR trap, beyond the maximum of the magnetic field at injection. This technique has an efficiency  $\epsilon$  of around 30%, while the ratio between metallic and buffer gas ions in the plasma is  $1 \div 10\%$ . For the PANDORA trap a dedicated resistive oven based on the Standard Temperature Oven (STO) has been developed at GSI. The STO has been being in operation at GSI for the production of metallic ion beams from the 14.5 GHz CAPRICE-type ECR Ion Source for several years. It can withstand up to 1,550°C to create vapours of metallic elements with high efficiency, low material consumption and longer lifetime Tinschert et al. [19]. However, in order to adapt the STO to the PANDORA Trap, some mechanical components have been modified. The system of three concentric stainless steel tubes for cooling water flow together with the inner insulated rod for the current connection made of alumina have been modified in order to



**FIGURE 9** | Sputtering system for the PANDORA trap.

get a 360–400 mm longer STO. This assembled part compensates the longer path to the plasma with respect to the plasma chamber of the CAPRICE ECRIS which the oven was designed for. Two complete longer STOs have been assembled and test have been carried out to check the water cooling flow, the vacuum, and the electrical connections. The items are ready for the shipment to INFN-LNS, where a test campaign has been scheduled with the AISHA ECRIS in order to study for the first time the performance of the STO with a 18 GHz ECRIS. For this purpose the injection flange of the AISHA ECRIS has been modified to match the oven feedthrough with the oven head. Since the STO has been designed and optimized for the CAPRICE-Type 14.5 GHz ECRIS, several evaporation tests will be carried out with metallic elements already produced at GSI, like Zn and Fe. After this feasibility tests, a campaign focused on the evaporation of isotopes like  $^{176}\text{Lu}$  and  $^{133}\text{Cs}$  will be scheduled. The study of the position and the insertion of the STOs into the PANDORA Trap together with the mechanical constrains is already ongoing. Ejection of neutral particles towards the plasma is obtained by employing the sputtering technique, normally used for refractory elements. A target of the material to be sputtered is prepared, mounted on a rod inside the magnetic trap and polarized negatively at some hundreds of V with respect to the plasma (sputtering voltage). The sputtering voltage accelerates ions naturally leaking from the core of the plasma to the target, causing the emission of neutral particles from it. Such neutral particles can be captured by the plasma but with a lower efficiency compared to the oven ( $\epsilon \leq 10\%$ ), due to the fact that they are ejected at an energy of several eVs. Normally, the ratio between sputtered ions and buffer gas ions is around 1%. The PANDORA trap will be equipped with a sputtering system built by the Pantechnik company PK [20] and shown in **Figure 9**: a rod with the sample to be sputtered is mounted inside a position adjuster allowing its movement under vacuum, in order to find the best operating position with respect to the plasma. The translation is transmitted to the rod through an insulated belt: this will allow connecting the sputtering system to the magnetic trap put at high voltage, while keeping its control at ground potential.

Among all the possible elements to be tested in PANDORA, three have been selected as first day experiments: they are listed

**TABLE 3** | List of elements selected for the first day experiments.

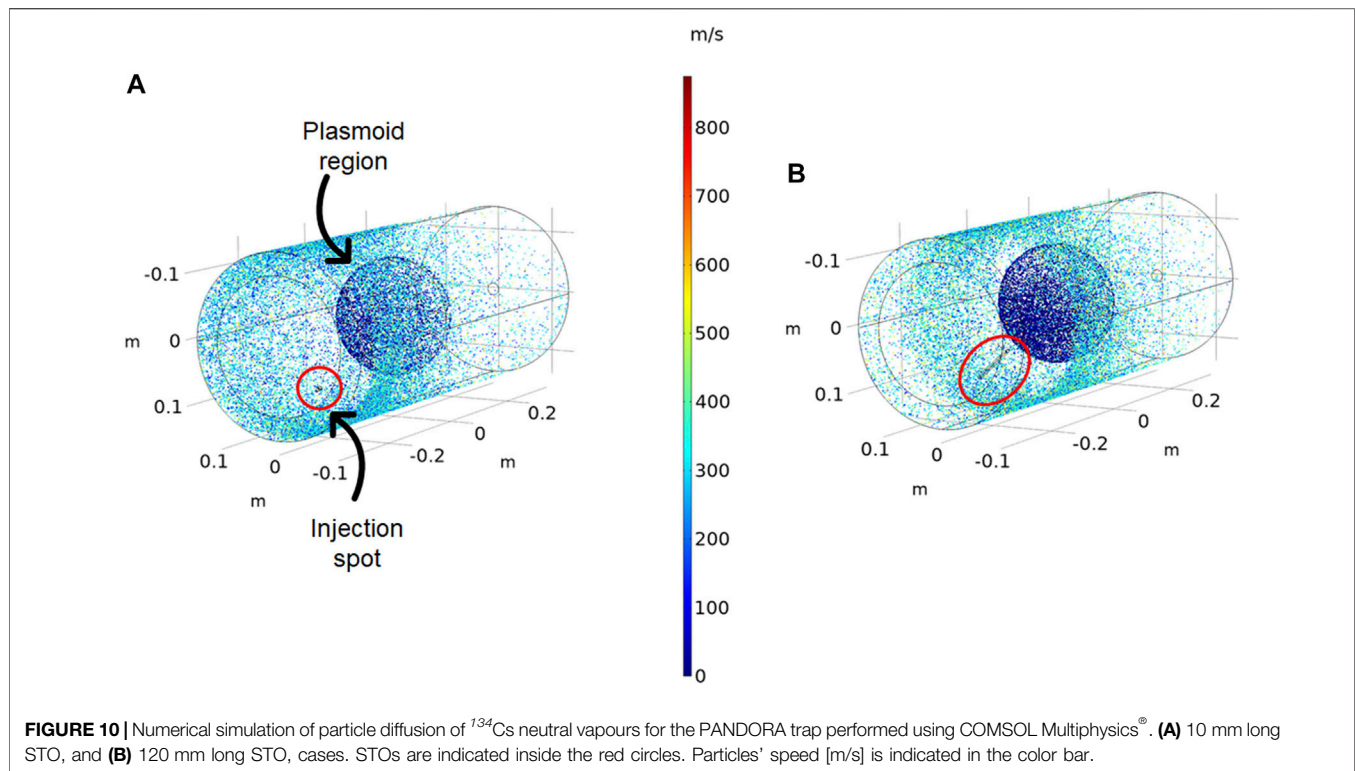
Isotope	Activity [GBq]	Consumption [mg]	Technique
$^{176}\text{Lu}$	4.246	2.00E+3	Oven
$^{134}\text{Cs}$	0.022	5.54E-10	Oven
$^{94}\text{Nb}$	0.173	2.46E-5	Sputtering

in **Table 3**, together with the necessary activity, the consumption for a single experiments and the technique will be employed to inject them into the plasma. Considering that the variation of the half life will be measured from the signal coming from the  $\gamma$  ray accompanying the  $\beta$  decay and that its detection should be distinguished by the background normally emitted by the plasma, the activity and the following consumption has been derived from the expected counting rate and measurement time necessary for the signal to overcome the  $3\sigma$  noise level coming from the background.

$^{176}\text{Lu}$  is commercially available with an enrichment of around 70%, but in oxide form. For this reason, before loading it inside the oven, reduction to metallic form will have to be applied. Test on the efficiency and cleanliness of the reduction process will be carried out on natural abundance Lu, in collaboration with the target Laboratory of INFN-LNL.  $^{134}\text{Cs}$  is commercially available as well, but in liquid solution of CsCl in HCl: for this reason, before loading it into the oven, a specific technique will be applied, currently adopted to produce  $^{133}\text{Cs}$  ion beams in the framework of the SPES project Galatà et al. [21]. The solution will be dried and the remaining compound will be loaded inside the resistive oven: heated under vacuum inside the trap at moderate temperatures ( $< 500^\circ\text{C}$ ), the compound will sublime and cesium dissociate, making it available for ionization by plasma electrons.  $^{94}\text{Nb}$  is available from several suppliers, as well as a product of nuclear reactors and the sputtering targets will be prepared using the technique employed with the negative ion sources for Tandem accelerators: a powder or small pieces of the material will be pressed in a metallic holder, that will then be screwed on the sputtering rod shown in **Figure 9**.

## 5.1 Numerical Simulations of Vapour Diffusion

In view of the aforementioned experimental campaign, we make some progress on the study of neutral vapour diffusion inside the PANDORA chamber. This aspect is relevant both for the optimization of the amount of material which turns into plasma state over the totality of the sample evaporated, and for studying the impact of deposited neutrals on the HpGe detection efficiency. The numerical study has been performed by means of COMSOL Multiphysics® with the purpose to study the diffusion of  $^{134}\text{Cs}$  neutral atoms in the cylindrical trap. First, we have checked under which fluid dynamic regime to study the problem. The Knudsen number,



$Kn = \lambda/L$ , can help in this sense. It is defined as the ratio of the species mean-free path length,  $\lambda$ , to a representative physical length scale, such as the chamber length  $L$ , which determines whether statistical mechanics or the continuum mechanics formulation of fluid dynamics should be used in the model. Considering some Cs neutral vapour parameters, in particular: pressure  $p \sim 10^{-5}$  mbar, temperature  $T_g = 417$  K, and the Cs particle diameter  $d_g \sim 6 \cdot 10^{-10}$  m, as well as a chamber length  $L = 700$  mm, the Knudsen number is around  $Kn \approx 7$ . Thus, the problem can be modelled in the *free molecular regime*, where collisions between gas molecules as they traverse the interior of the system can be ignored.

As mentioned before, the STO head position can be longitudinally adjusted by using a rod that allows to expose it outside of the injection flange, towards the center of the plasma chamber. Two STOs of, respectively, 10 and 120 mm length have been employed for the neutral vapour tracing simulations: results are visible in **Figure 10A** for the 10 mm-long STO and in **Figure 10B** for the 120 mm-long STO. The not-axisymmetric position of STOs is required to avoid the magnetic branches location on the injection plate, as shown in **Figure 6**. The STOs are also tilted with respect to the chamber axis in order to maximize the injection direction towards the center of the plasma chamber. Vapours have starting velocity conditions according to a Maxwellian distribution with an initial temperature  $T = T_g$ , and the particles' speed is indicated in the color bar in the figure. The emitting surface radius of the STO is 2.5 mm. Modelled particles' trajectory drifts according to the initial conditions, until they hit the chamber

walls or the modelled plasmoid surface (in middle of the chamber). Particles hitting the wall surface have non zero probability to be re-emitted since the surface temperature is close to  $T_g$ . This was assumed trying to simulate the effects of an internal liner on the surface. Moreover, particles hitting the plasmoid surface have about 6% probability to pass through, and hence about 94% probability to stick on the surface. These numbers arises from mean-free path calculations of neutral atoms going into ionization, at a given average electron density and ionization cross section. Particles sticking on the plasmoid are assumed to go into plasmization. As can be evinced, depositions of **Figure 10B** compared to that of **Figure 10A** is different. Because of the closer position of STO emitting surface of the former, a greater neutral deposition in the central region of the chamber is achieved, which is closer to the plasmoid; conversely, a more broadened deposition is shown in the latter case, where most of neutrals end close to the injection position. Therefore, the longer STO seems to provide a better chance for the neutrals to interact with the plasma, hence more likely being ionized by the warm electron population, and to a less waste of evaporated material. The calculated ratio of particle deposited on the plasmoid over the total amount of particles (i. e., deposited both on the plasmoid and on the chamber wall) is 17 and 30% for **Figures 10A,B**, respectively. Further investigations on the problem are planned, including space-dependent plasma parameters in the neutral atoms ionization mechanism, which we expect to impact on the deposition map of remaining neutrals. These preliminary results have been used to study the HPGe detectors efficiency as a function of vapour deposition Naselli et al. [8].

## 6 CONCLUSION

In this work the numerical design of the PANDORA magnetic system, for plasma confinement, has been presented. The design, whose scaling is based on the employment of 18 and 21 GHz pumping frequencies, has been carried out by using the commercial simulators OPERA and CST, whose results are in agreement between each other. By employing the obtained magnetic field profiles, the positions of the magnetic branches have been identified. These positions, along the plasma chamber side walls, are critical due to generated strong Bremsstrahlung radiation and need to be avoided when placing the array of  $\gamma$ -ray detectors. Furthermore, the lost electron maps on the plasma chamber end plates have been calculated through the magnetic field profile: this information will be relevant both for the design of the bias-disk (at the injection end-plate) and for the correct placement of the plasma chamber diagnostics. The second part of the work has been dedicated to the numerical simulation of the microwave injection system: it will be composed by two 2.4 kW WR62 waveguides ( $f_{RF} = 18$  GHz) and one 1.5 kW WR51 waveguide ( $f_{RF} = 21$  GHz), for a total of 6 kW total available power. First in-vacuum simulations show that, with the proposed configuration, the waveguide ports cross-talk is minimized ( $|S_{ij}| < -10$  dB) and a high number of well adapted modes is excited inside the empty cavity, that is desirable to exploit the frequency tuning effect in order to improve source performances. The last part of the work deals about the techniques to inject the elements of interest inside the magnetic trap. Because PANDORA experiments will employ radioactive isotopes, available in limited amount and at a high cost, efficient injection techniques, in terms of atoms percentage and speed of

preparation, need to be implemented and are discussed. Finally, preliminary COMSOL simulations have been performed to study the neutral vapour diffusion inside the plasma chamber: this is relevant both for the optimization of the amount of material which turns into plasma state over the totality of the sample evaporated, and for studying the impact of deposited neutrals on the HPGe detection efficiency.

## DATA AVAILABILITY STATEMENT

The original contributions presented in the study are included in the article/Supplementary material, further inquiries can be directed to the corresponding author.

## AUTHOR CONTRIBUTIONS

Conceptualization, GM, LC, DM, and GT, Numerical simulations, GM, GT, AP, AG, EN, MM, and FR, Isotopes injection studies, AG, FM, RL, and KT, Funding acquisition, DM and DS, Writing—original draft, GM, Writing—review and editing, GM, GT, AP, AG, FM, and DM. All authors have read and agreed to the published version of the manuscript.

## ACKNOWLEDGMENTS

The authors wish to thank INFN for the support through the project PANDORA Gr3 funded by 3rd Nat. Sci. Comm., and to thank the whole PANDORA collaboration.

## REFERENCES

- Mascali D, Santonocito D, Amaducci S, Andò L, Antonuccio V, Biri S, et al. A Novel Approach to  $\beta$ -Decay: PANDORA, a New Experimental Setup for Future In-Plasma Measurements. *Universe* (2022) 8:80. doi:10.3390/universe8020080
- Geller R. *Electron Cyclotron Resonance Ion Sources and ECR Plasmas*. London, UK: Institute of Physics (1996).
- Gammino S, Ciavola G. The Role of Microwave Frequency on the High Charge States Buildup in the ECR Ion Sources. *Plasma Sour Sci. Technol.* (1996) 5: 19–27. doi:10.1088/0963-0252/5/1/002
- Leitner D. High Performance ECR Sources for Next-Generation Nuclear Science Facilities. In: 10th International Particle Accelerator Conference. WEXPLS1 (2019). doi:10.18429/JACoW-IPAC2019-WEXPLS1
- Benitez J, Lyneis C, Phair L, Todd D, Xie D. Dependence of the Bremsstrahlung Spectral Temperature in Minimum-B Electron Cyclotron Resonance Ion Sources. *IEEE Trans Plasma Sci* (2017) 45:1746–54. doi:10.1109/tps.2017.2706718
- Mazzaglia M, Castro G, Mascali D, Miracoli R, Briefi S, Fantz U, et al. Study of the Influence of Magnetic Field Profile on Plasma Parameters in a Simple Mirror Trap. In: Proc. 23rd International Workshop on ECR Ion Sources (ECRIS'18); 10–14 September 2018; Catania, Italy. Geneva, Switzerland: JACoW Publishing (2019). p. 144–7. no. 23 in International Workshop on ECR Ion Sources. doi:10.18429/JACoW-ECRIS2018-TUP25
- Neben D, Fogleman J, Isherwood B, Leitner D, Machicoane G, Renteria S, et al. X-ray Investigation on the Superconducting Source for Ions (SuSI). *J Inst* (2019) 14:C02008. doi:10.1088/1748-0221/14/02/c02008
- Naselli E, Santonocito D, Amaducci S, Galatà A, Goasduff A, Mauro GS, et al. Design Study of a HPGe Detectors Array for  $\beta$ -decays Investigation in Laboratory ECR Plasmas. *Front Phys* (2022). Research Topics: Nuclear Physics and Astrophysics in Plasma Traps (forthcoming).
- Mascali D, Neri L, Gammino S, Celona L, Ciavola G, Gambino N, et al. Plasma Ion Dynamics and Beam Formation in Electron Cyclotron Resonance Ion Sources. *Rev Scientific Instr* (2010) 81:02A334. doi:10.1063/1.3292932
- Gammino S, Ciavola G, Celona LG, Mascali D, Maimone F. Numerical Simulations of the Ecr Heating with Waves of Different Frequency in Electron Cyclotron Resonance Ion Sources. *IEEE Trans Plasma Sci* (2008) 36:1552–68. doi:10.1109/tps.2008.927288
- Hitz D, Girard A, Melin G, Gammino S, Ciavola G, Celona L. Results and Interpretation of High Frequency Experiments at 28 Ghz in Ecr Ion Sources, Future Prospects. *Rev Scientific Instr* (2002) 73:509–12. doi:10.1063/1.1429313
- Zhao HW, Sun LT, Guo JW, Lu W, Xie DZ, Hitz D, et al. Intense Highly Charged Ion Beam Production and Operation with a Superconducting Electron Cyclotron Resonance Ion Source. *Phys Rev Accel Beams* (2017) 20: 094801. doi:10.1103/PhysRevAccelBeams.20.094801
- Xie D, Benitez J, Lu W, Lyneis C, Todd D. Recent Production of Intense High Charge Ion Beams with VENUS. In: 22nd International Workshop on ECR Ion Sources. THAO01 (2017). doi:10.18429/JACoW-ECRIS2016-THAO01
- Guo JW, Sun L, Lu W, Zhang WH, Feng YC, Shen Z, et al. A New Microwave Coupling Scheme for High Intensity Highly Charged Ion Beam Production by High Power 24–28 GHz SECRAL Ion Source. *Rev Scientific Instr* (2020) 91: 013322. doi:10.1063/1.5131101
- Mauro GS, Torrisi G, Leonardi O, Pidotella A, Sorbello G, Mascali D. Design and Analysis of Slotted Waveguide Antenna Radiating in a "Plasma-Shaped"

- Cavity of an ECR Ion Source. *Telecom* (2021) 2:42–51. doi:10.3390/telecom2010004
16. Vondrasek R. Diagnostics for Multiple Frequency Heating and Investigation of Underlying Processes. *Rev Scientific Instr* (2022) 93:031501. doi:10.1063/5.0076265
  17. Lyneis CM, Leitner D, Todd DS, Sabbi G, Prestemon S, Caspi S, et al. Fourth Generation Electron Cyclotron Resonance Ion Sources (Invited). *Rev Sci Instrum* (2008) 79:02A321. doi:10.1063/1.2816793
  18. Brown IG. *The Physics and Technology of Ion Sources, 2nd, Revised and Extended Edition*. Hoboken, NJ, USA: Wiley (2004).
  19. Tinschert K, Lang R, Mäder J, Maimone F, Roßbach J. Metal Ion Beam Production with Improved Evaporation Ovens. In: Proceedings of the 20th International Workshop on ECR IonSources; September 25–28 (2012). p. 140–2.
  20. [Dataset] Pantechnik. *Pantechnik* (2022). Available from: [www.pantechnik.com](http://www.pantechnik.com) (Accessed June 20, 22).
  21. Galatà A, Roncolato C, Bisoffi G, Francescon P, Bellan L, Bermudez J, et al. Towards the First Beams from the ADIGE Injector for the SPES Project. *J Phys Conf Ser* (2019) 1350:012090. doi:10.1088/1742-6596/1350/1/012090

**Conflict of Interest:** The authors declare that the research was conducted in the absence of any commercial or financial relationships that could be construed as a potential conflict of interest.

**Publisher's Note:** All claims expressed in this article are solely those of the authors and do not necessarily represent those of their affiliated organizations, or those of the publisher, the editors and the reviewers. Any product that may be evaluated in this article, or claim that may be made by its manufacturer, is not guaranteed or endorsed by the publisher.

Copyright © 2022 Mauro, Celona, Torrisi, Pidatella, Naselli, Russo, Mazzaglia, Galatà, Maimone, Lang, Tinscher, Santonocito and Mascali. This is an open-access article distributed under the terms of the Creative Commons Attribution License (CC BY). The use, distribution or reproduction in other forums is permitted, provided the original author(s) and the copyright owner(s) are credited and that the original publication in this journal is cited, in accordance with accepted academic practice. No use, distribution or reproduction is permitted which does not comply with these terms.